Saad Misfer Al-Qahtani*, Galyna Bryzgalova, Ismael Valladolid-Acebes, Marion Korach-André, Karin Dahlman-Wright, Suad Efendić, Per-Olof Berggren and Neil Portwood

17β-Estradiol suppresses visceral adipogenesis and activates brown adipose tissue-specific gene expression

DOI 10.1515/hmbci-2016-0031
Received June 15, 2016; accepted September 30, 2016; previously published online November 10, 2016

Abstract: Both functional ovaries and estrogen replacement therapy (ERT) reduce the risk of type 2 diabetes (T2D). Understanding the mechanisms underlying the antidiabetic effects of 17β-estradiol (E2) may permit the development of a molecular targeting strategy for the treatment of metabolic disease. This study examines how the promotion of insulin sensitivity and weight loss by E2 treatment in high-fat-diet (HFD)-fed mice involve several anti-adipogenic processes in the visceral adipose tissue. Magnetic resonance imaging (MRI) revealed specific reductions in visceral adipose tissue volume in HFD+E2 mice, compared with HFD mice. This loss of adiposity was associated with diminished visceral adipocyte size and reductions in expression of lipogenic genes, adipokines and of the nuclear receptor *nr2c2/tr4*. Meanwhile, expression levels of adipose triglyceride lipase/*pnpla2* and leptin receptor were increased. As mRNA levels of *stat3*, a transcription factor involved in brown adipose tissue differentiation, were also increased in visceral adipose, the expression of other brown adipose-specific markers was assessed. Both expression and immunohistochemical staining of *ucp-1* were increased, and mRNA levels of *dio-2*, and of *adrβ3*, a regulator of *ucp-1* expression during the thermogenic response, were increased. Furthermore, expression of *cpt-1b*, a brown adipose-specific gene involved in fatty acid utilization, was also increased. Methylation studies demonstrated that the methylation status of both *dio-2* and *adrβ3* was significantly reduced. These results show that improved glycemic control and weight loss due to E2 involve anti-adipogenic mechanisms which include suppressed lipogenesis and augmented fatty acid utilization, and in addition, the activation of brown adipose tissue-specific gene expression in association with E2-dependent epigenetic modifications in these genes.

Keywords: adipogenesis; β3-adrenergic receptor; brown fat; *cpt-1b*; *dio-2*; E2; epigenetic; 17β-estradiol; insulin resistance; menopause; methylation; Nr2c2/tr4; obesity; *ucp-1*; Visceral fat.

***Corresponding author: Saad Misfer Al-Qahtani,** The Rolf Luft Research Center for Diabetes and Endocrinology, Karolinska Institutet, Karolinska University Hospital L1, SE-171 76 Stockholm, Sweden; Departments of Molecular Medicine and Surgery, Karolinska Institute, Karolinska University Hospital, SE-171 76 Stockholm, Sweden; and Department of Pathology, College of Medicine and Najran University Hospital, Najran University, 61441, Najran, Saudi Arabia, E-mail: saad.alqahtani@ki.se
Galyna Bryzgalova, Ismael Valladolid-Acebes, Per-Olof Berggren and Neil Portwood: The Rolf Luft Research Center for Diabetes and Endocrinology, Karolinska Institutet, Karolinska University Hospital L1, SE-171 76 Stockholm, Sweden
Marion Korach-André: Metabolism Unit, and KI/AZ Integrated CardioMetabolic Center, Department of Medicine Karolinska Institutet at Karolinska University Hospital Huddinge, C2-84, S-141 86 Stockholm, Sweden
Karin Dahlman-Wright: Department of Biosciences and Nutrition, Novum, Karolinska Institutet, S-141 83 Huddinge, Sweden
Suad Efendić: Departments of Molecular Medicine and Surgery, Karolinska Institute, Karolinska University Hospital, SE-171 76 Stockholm, Sweden

Introduction

Menopause is associated with the development of increased abdominal fat mass [1], whilst the presence of central adiposity, a parameter which includes abdominal fat, is a predictor for risk of type 2 diabetes (T2D) [2]. In pre-menopausal women, T2D frequency is less than in men [3], and estrogen replacement therapy (ERT) reduces T2D incidence [4], suggesting that ovarian function protects against T2D. As ERT is associated with adverse events such as breast cancer and stroke, understanding the mechanisms which underlie the benefits of 17β-estradiol (E2) may permit their targeting and avoid ERT's undesirable effects.

In rodents, ablation of E2 signaling by ovariectomy or by loss of the estrogen receptor (ER) α or aromatase genes (ERKO and ARKO mice, respectively) leads to weight gain, increased adiposity, adipocyte hypertrophy and

altered adipokine levels [5–7]. In ovariectomized mice, E2 treatment reverses these changes [8] and promotes weight loss and insulin sensitivity in models of T2D [9]. The sites of action of E2 include the hypothalamus and peripheral organs such as the adipose tissue. In the hypothalamus, silencing of ERα leads to hyperphagia, adiposity, reduced energy expenditure and glucose intolerance [10]. However, although the effects of E2 on body weight involve the regulation of food intake [11], ovariectomy increases adiposity even after pair-feeding [12], and ERKO and ARKO mice are obese in the absence of increased feeding [5, 6]. Indeed, E2 administration in ovariectomized mice leads to increased energy expenditure [10]. Thus, it is likely that the suppression of body weight by E2 involves mechanisms in addition to the regulation of feeding.

In adipose tissue, the anti-adipogenic effects of E2 involve the promotion of lipolysis [13] and the decreased expression of lipogenic genes [9]. The transcription factor sterol regulatory element binding protein 1c (SREBP1) is a principal regulator of lipogenic gene expression [14] and in the adipose, *srebp1* is suppressed by liver X receptor alpha (*lxrα*) [15]. However, the nuclear receptor, testicular receptor (*tr4*), also known as *nr2c2*, has recently been identified as a potentially important regulator of stearoyl-CoA desaturase 1 (*scd1*) expression [16]. Furthermore, in addition to the anti-adipogenic role attributed to ERα, signaling through ERβ decreases proliferator-activated receptor gamma (PPARγ) activity, suppressing its downstream insulin-sensitizing effects and activation of lipogenic pathways [17]. Finally, E2 controls the expression of both signal transducer and activator receptor 3 (*stat3*) [18], a regulator of brown adipocyte differentiation and function [19], and of the β-3 adrenergic receptor (*adrβ3*), which regulates the thermogenic response in the brown adipose tissue [20].

To understand the complex events linking E2 signaling with weight loss and improved insulin sensitivity, we investigated changes in body weight, adipose depot volume and adipocyte morphology, and the accompanying alterations in gene expression, in E2-treated mice fed on a high-fat diet (HFD). As epigenetic changes may underlie the connection between environmental factors and the genetic alterations associated with obesity and insulin resistance, we also examined the methylation status of genes regulated by E2 in HFD mice. The results show that the promotion of glycemic control by E2 is associated with the suppression of adipogenicity and the activation of brown adipose tissue-specific gene expression in association with E2-dependent epigenetic modifications in these genes.

Materials and methods

Animals, treatment and tissue processing

Seven-week-old female C57BL/6J mice (Scanbur BK, Sweden) were housed at 22 °C–23 °C in a 12 h-12 h light-dark cycle with free access to water and food ad libitum. Mice were acclimatized for 1 week and divided randomly for maintenance on either a low-fat diet (LFD; 4.5 g fat/100 g; Lactamin, Sweden) or a high-fat diet (HFD; 34.9 g fat/100 g; D12492, Research Diets, USA) until 12 months of age [9]. At 11 months of age, both groups were divided for subcutaneous injection for 30 days with either 50 μg/kg/day E2 (Sigma-Aldrich, Sweden; LFD+E2 and HFD+E2 mice) prepared in vehicle or with the same volume of vehicle (sesame oil/ethanol, 9:1; LFD, HFD mice). Body weight and food consumption were measured at the start of treatment and thereafter at 48-h intervals. Tissues were collected from overnight-fasted, euthanized mice, snap-frozen and stored at −80 °C. All procedures were approved by the local Ethical Committee.

Intraperitoneal glucose tolerance test (IPGTT)

Mice were fasted overnight, and blood glucose levels were assessed by a glucometer (MediSence, Abbott Scandinavia, Solna, Sweden) before, and at 30, 60 and 120 min following an intraperitoneal injection of glucose (2 g/kg body weight).

Plasma insulin levels

Insulin levels in plasma were determined by using an AlphaLISA kit (Perkin-Elmer, Sweden), according to the manufacturer's protocol.

Magnetic resonance imaging (MRI)

For in vivo MRI, LFD, HFD and HFD+E2 mice were anesthetized with 1.5%–2.0% isoflurane in O_2 while positioned on a heated pad over which a current of air heated to 37 °C was passed to further maintain the body temperature. Fat distribution measurements were performed on a Bruker 4.7-T field strength magnet and a 40-cm horizontal-bore diameter (Bruker Biospec Avance 47/40; Bruker, Karlsruhe, Germany), equipped with a commercially available circular resonator (Bruker) with an inner diameter of 24 mm for RF pulse application and signal detection using a rapid acquisition with relaxation enhancement (RARE) imaging sequence. MRI was performed to acquire a total of 29–34 contiguous 1.5 mm thick transverse slices, corresponding to the thoracic to pelvic regions. Output image series were collected in Paravision 3.01 (Bruker) and exported to ImageJ (1,47v, Wayne Rasband, NIH, USA) for calculation by cumulative pixel analyses of total body volume and volumes of the visceral and subcutaneous fat depots. Comparable ranges of consecutive slices were analyzed for all individuals. A signal threshold was used after a Gauss filter of maximum likelihood, and a class-select interaction was applied to exclude all non-fat tissues in each slice. Results are expressed as a percentage of body volume.

Histology and immunohistochemistry (IHC)

For histology, three sections of 20 µm thickness were cut from adipose tissue from three mice per group by cryostat. The sections were stained with hematoxylin and eosin, and three images per section were collected using a digital camera (10× and 40× magnifications, Leica DM 3000 LED, LAS Version 4.3.0). Adipocyte size was quantified in 80–170 cells per section by ImageJ (1,47v, Wayne Rasband, NIH, USA).

For IHC, sections of 20 µm thickness were prepared from acetone-fixed adipose tissue and blocked with 5% rabbit serum in antibody diluent (Cell Signaling Technology) for 1 h at room temperature. After blocking, the sections were incubated with anti-uncoupling protein 1 (UCP1) antibody (Abcam, UK; 250× dilution in antibody diluent) overnight at 4 °C. After three washes with Tris-buffered saline (TBS), the sections were incubated with horseradish peroxidase (HRP)-conjugated goat anti-rabbit IgG polyclonal antibody (Abcam; 1000× dilution in antibody diluent). Immunostaining was enhanced by the use of diaminobenzidine. After counterstaining with hematoxylin, the sections were treated with ethanol and xylene prior to mounting. All of these steps included negative controls, which consisted of similarly treated sections except that the primary antibody was omitted. Three images per section were collected using a digital camera (10× and 40× magnification, Leica DM 3000 LED, LAS Version 4.3.0).

Western blotting

Snap-frozen adipose tissue was homogenized in radioimmunoprecipitation assay (RIPA) buffer and centrifuged for 30 min at 12,000 *g* and 4 °C. The supernatants were collected, and the protein concentrations were assayed according to a standard assay protocol (DC protein assay, Bio-Rad, USA). Protein samples were run on 10% ECL gels (Amersham, GE Healthcare, UK) and transferred to polyvinylidene difluoride (PVDF) membranes. The membranes were blocked for 1 h in 5% fat-free dry milk (Bio-Rad Laboratories, Sweden) dissolved in TBS, and the membrane was washed once with wash buffer [TBS/0.1% (v/v) Tween-20]. Primary antibody (Table 1) was added in a 10 mL volume of TBS buffer, and the incubation was continued overnight at 4 °C. The membranes were then washed and incubated with secondary antibody in 10 mL of TBS for 1 h at room temperature, according to the manufacturer's recommendations (Table 1). After three further washes with wash buffer, bands were visualized using an ECL detection kit (SuperSignal West Femto, Thermo Scientific Pierce, Nordic Biolabs Sweden) and documented using a LAS 3000 system (Fuji Film Co., Tokyo, Japan). Band intensities were quantified employing ImageJ.

RNA preparation and real-time RT-PCR

Total RNA was prepared using RNeasy Lipid kits and treated with DNase I (Qiagen, Sweden), and reverse-transcribed using TaqMan® Reverse Transcription Reagents and random hexamer primers (Applied Biosystems, Sweden). All target mRNAs were assayed in triplicate 25 µL reactions which included the respective Assay-on-Demand (Table 2) and 1× Master Mix (both from Applied Biosystems, Sweden) using a 7300 Real-Time PCR system. Expression levels were normalized to 18S (Applied Biosystems, Sweden). Fold changes in target gene expression were determined by the Δ-Δ C_T method.

DNA preparation and methylation analysis

Genomic DNA was extracted from adipose tissue using a PureLink® Genomic DNA Mini Kit (Thermo Fisher Scientific, Sweden), according to the manufacturer's protocol for mammalian tissues. Analysis of methylation was carried out using an OneStep qMethyl Kit (Zymo Research, Irvine, CA, USA). Aliquots of 280 ng of each sample of DNA were placed into test and reference reactions containing 28 µL of 2×Test/Reference Reaction Premix in a final volume of 140 µL. The Test Reaction Premix contains methylation sensitive restriction enzymes, while the Reference Reaction Premix does not. All the samples were incubated for 5 h at 37 °C, after which 7 µL aliquots of each test and reference reaction were employed as template for duplicate 25 µL real-time PCR reactions containing 2×SYBR Green Master Mix (Applied Biosystems, Sweden) and 50 nM of each primer of interest (Thermo Fisher Scientific, Sweden; Table 3). The primers employed were designed using the web-based primer design tool Primer3. Primer pairs were designed to amplify the mouse homologues of regions which include CpG13S in the human SCD1 promoter [21], CpG48-50 in the human FASN promoter [21], methylation site #6 of the human CPT1b promoter [22] and regions amplified by the ADRB3 and DIO2 primers employed by Kurylowicz et al. [23]. The specificity of amplification of each primer pair was verified by initial melting curve analyses. Amplifications were carried out using a 7300 Real-Time PCR system. As positive and negative controls, aliquots of methylated and non-methylated genomic DNA (Zymo Research, Irvine, CA, USA) were subjected to parallel methylation-PCR analyses. The methylation level of the region of interest of each target gene was expressed as a percentage as determined using the following equation: methylation (%) = $100 \times 2^{-\Delta Ct}$. The ΔCt is the average Ct value of the test reaction minus the average Ct value of the reference reaction.

Statistical analyses

Data were analyzed using the Prism Graph Pad Software (CA, USA). All values are presented as mean ± SEM. Significances were calculated using analysis of variance (ANOVA), followed by the Bonferroni post hoc analysis with multiple comparisons. The values of $p < 0.05$ were considered significant.

Table 1: Antibodies and antibody dilutions used for Western blotting studies.

Antibody	Mol. wt (kDa)	Dilution factor	Manufacturer
Anti-Uncoupling protein 1 (UCP-1)	32	1 : 1000	Abcam
Nuclear receptor subfamily 2, group C, member (2Nr2c2/TR4) (ab109301)	62	1 : 1000	Abcam
Anti-rabbit IgG, HRP-linked Antibody(ab97051)	42	1 : 2000	Abcam

Table 2: mRNA targets and Assay-on-Demand designations used for RT-PCR studies.

Gene	Primer code	Full name
SCD1	Mm00772290_m1	Stearoyl-CoA desatturase 1
FAS	Mm00662319_m1	Fatty acid synthase
ACC1	Mm0130428_m1	Acetyl-CoA carboxylase
CD36	Mm01135198_m1	Fatty acid translocase
LXRα	Mm00443454_m1	Liver X receptor α
Pparα	Mm00440939_m1	Proliferator-activated receptor α
Pparγ	Mm00440945_m1	Proliferator-activated receptor γ
Stat-3	Mm00456961_m1	Signal transducer and activator receptor 3
SREBP1	Mm00550338_m1	Sterol regulatory element binding protein 1c
Lep	Mm00434759_m1	Leptin
Retn	Mm00445641_m1	Resistin
AdipoQ	Mm00456425_m1	Adiponectin
LepR	Mm00440174_m1	Leptin receptor
AdipoR1	Mm01291334_m1	Adiponectin receptor 1
AdipoR2	Mm01184028_m1	Adiponectin receptor 2
UCP-1	Mm01244861_m1	Uncoupling protein 1
PGC-1α	Mm1208835_m1	Peroxisome proliferator-activated receptor γ coactivator 1-α
DIO-2	Mm00515664_m1	Type II iodothyronine deiodinase
CIDEA	Mm00432554_m1	Cell death-inducing DNA fragmentation factor, α subunit-like effector A
Cox8b	Mm00432648_m1	Cytochrome c oxidase, subunit VIIIb
ADRβ3	Mm02601819_g1	β-3 adrenergic receptor
CPT-1b	Mm00487191_g1	Carnitine palmitoyltransferase 1b
Nr2c2/TR4	Mm01182440_m1	Nuclear receptor subfamily 2, group C, member 2
Pnpla2	Mm00503040_m1	Patatin-like phospholipase domain containing 2
LIPE	Mm00495359_m1	lipase, hormone sensitive
18S		Endogenous standard

Table 3: Primers used for the analysis of methylation status.

Gene	Oligo name	Primers	
ADRβ3	mADRB3 F738	F	5′CCCTACTGTCCCCTTCCCTA3′
	mADRB3 R1082	R	5′CTGGTGGCATTACGAGGAGT3′
DIO-2	mDIO2 F210	F	5′TCTCCA ACTGCCTCTTCCTG3′
	mDIO2 R433	R	5′TTCAGGATTGGAGACGTGCA3′
CPT-1b	mCPT1b F-253	F	5′CTCCTG GTGACCTTTTCCCT3′
	mCPT1b R-43	R	5′ACTTGACACCCACTCCCAAA3′
SCD1	mSCD1 F-830	F	5′ACTCAGGCCCTTTGATTCCT3′
	mSCD1 R-604	R	5′TGTATCCCTTCAGCCAGCAT3′
FAS	mFASN F-134	F	5′GCCCATCACCCTATTGCCTA3′
	mFASN R78	R	5′GGTCACACTGGAAACTCTGC3′

Results

Glucose tolerance, plasma insulin levels, body weight and food intake

HFD mice exhibited increased fasting glucose levels and impaired glucose tolerance (Figure 1A), in parallel with increased plasma levels of insulin (Figure 1B). E2 had no effects on glucose tolerance and insulin levels in LFD+E2 mice but suppressed both glucose and insulin levels in HFD+E2 mice to levels comparable with those in LFD mice (Figure 1A and B).

Compared with LFD mice, maintenance of mice on an HFD for 10 months led to significant increases in body weight (Figure 1C). E2 treatment resulted in reductions in the body weight of HFD+E2 mice from day 10 of treatment, compared to HFD mice, and by the end of E2 treatment, body weights in HFD+E2 mice were 74% of those of mice in the HFD group. In LFD+E2 mice, E2 treatment did not affect either body weight (Figure 1C) or food intake (Figure 1D). However, body weight changes in HFD+E2 mice were accompanied by decreases in food intake from 4 days of treatment; although these reductions were not significantly different at all time points (Figure 1D).

Body composition

As the effects of E2 on body weight may reflect alterations in adiposity, the volumes of the subcutaneous and visceral fat depots were quantified by MRI. LFD+E2 mice were not included in this study, as body weight was unchanged in

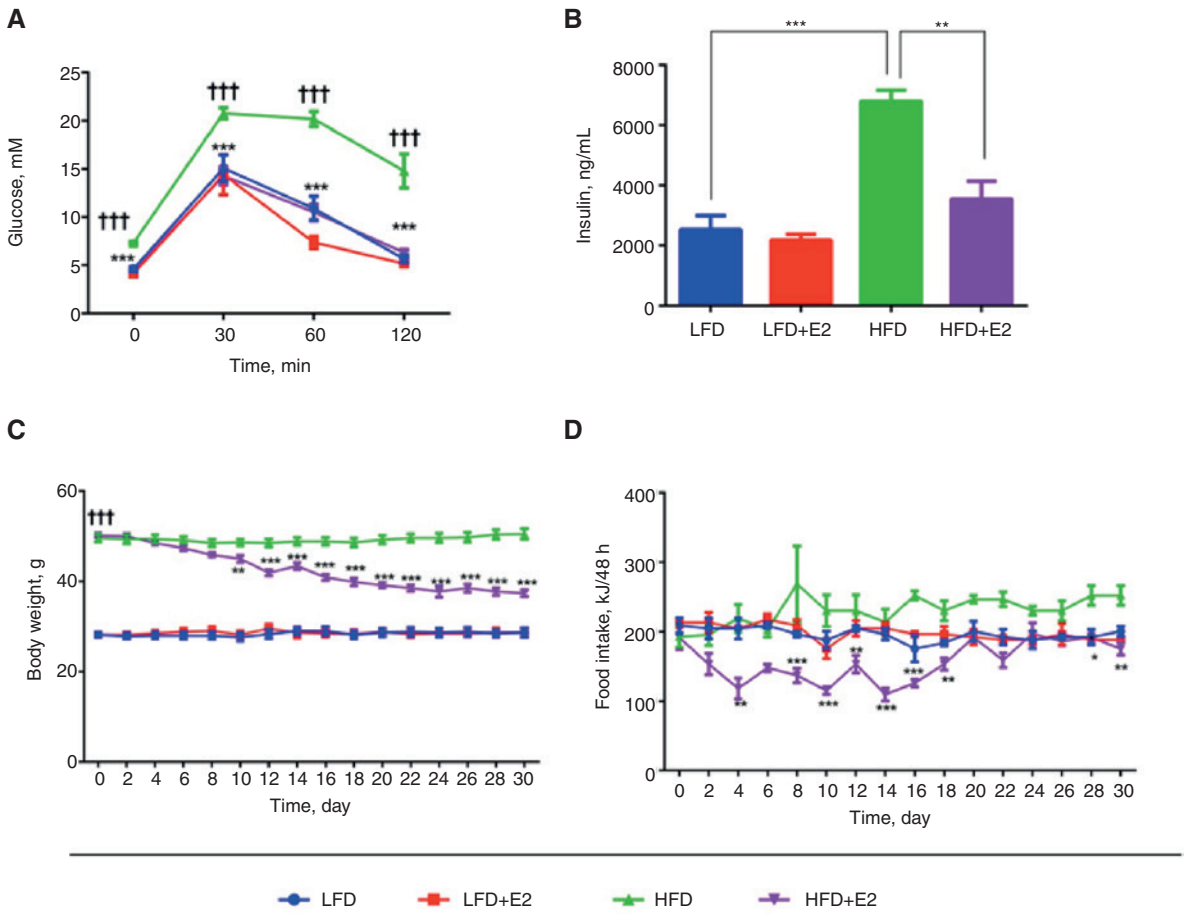

Figure 1: Intraperitoneal glucose tolerance test (IPGTT), plasma insulin levels, body weight and food intake in LFD and HFD mice treated with E2 or vehicle.
(A) Levels of blood glucose were determined before and after administration of a glucose load (2 g/kg body wt ip) at the indicated time points. †††, p-value < 0.001 for HFD vs. LFD and ***, p-value < 0.001 for HFD+E2 vs. HFD. (B) Plasma insulin levels. ***, p-value < 0.001 for HFD vs. LFD and **, p-value < 0.01 for HFD+E2 vs. HFD. (C) and (D) Body weight and food intake, respectively, were measured before and at 48-h intervals during treatment of mice that were housed in pairs. Body weight in HFD mice is significantly higher than that of LFD mice at all time points. †††, p-value < 0.001 for HFD vs. LFD while *, p-value < 0.05, **, p-value < 0.01 and ***, p-value < 0.001 for HFD+E2 vs. HFD mice; n = 6–8 mice in (A) and (C), and 3–4 mice in (B) and (D).

this group (Figure 1C). E2 treatment led to a non-significant reduction in subcutaneous adipose volume (Figure 2A, B). However, the volume of the visceral adipose depot was significantly increased in HFD mice, and in HFD+E2 mice, the volume of this depot decreased to 67% of that of the HFD group (Figure 2A, C).

Visceral adipocyte morphology

As the reductions in the visceral adipose volume in HFD+E2 mice correlated with body weight reduction, we studied the effects of E2 in this depot. Changes in adipose tissue volume may be due to alteration in adipocyte size, and morphological analyses showed that visceral adipocyte size in HFD mice was 2.2 times greater than that of LFD mice (Figure 2D, E). In HFD+E2 mice, adipocyte size was reduced 2-fold by E2 treatment (Figure 2D, E), suggesting that E2 treatment in HFD+E2 mice reduced body weight and central adiposity in association with a hypotrophic effect on the visceral adipocyte population.

Gene expression and protein levels in visceral adipose tissue

As adipocyte hypertrophy is associated with an increase in the ratio of lipid deposition to lipolysis, the expression of genes involved in lipogenesis, fatty acid uptake and lipolysis was studied in the visceral adipose. Transcript

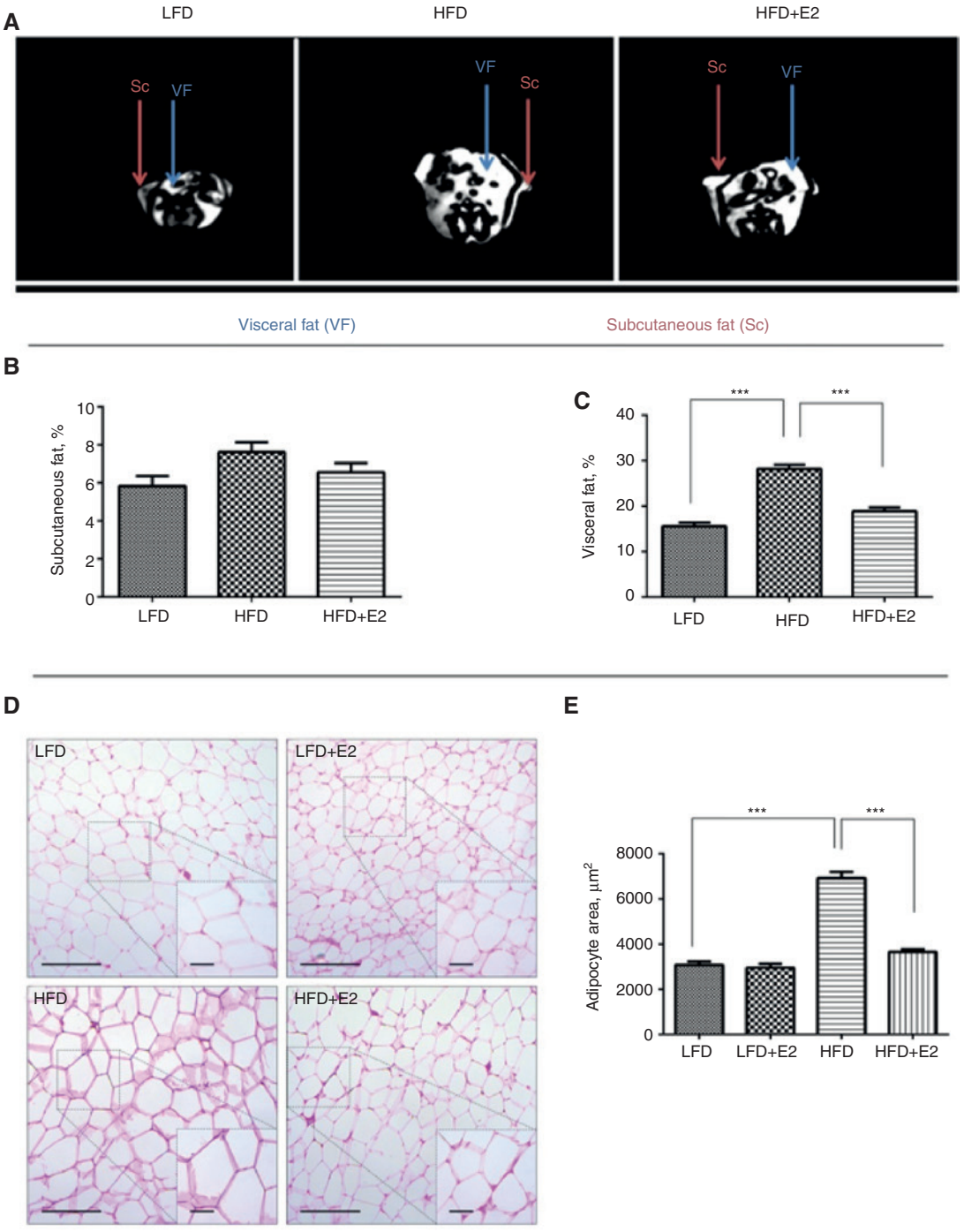

Figure 2: Magnetic resonance imaging (MRI) and visceral adipocyte morphology in LFD mice, and HFD mice treated with E2 or vehicle. (A) Representative axial MRI images of the abdominal region in LFD mice, and in the vehicle- and E2-treated HFD mice. Arrows indicate visceral (VF) and subcutaneous (Sc) fat depots. (B) and (C) Volumes of the subcutaneous and visceral adipose depots, respectively, presented as the percentage of total body volume. (D) Hematoxylin and eosin-stained sections were prepared from dissected visceral adipose of vehicle- or E2-treated LFD and HFD mice; representative images from each group are shown at 10× and 40×. (E) Adipocyte area was calculated from three hematoxylin and eosin-stained sections per group. ***, p-value < 0.001; n = 6 mice in (B) and (C), and n = 3 mice in (D) and (E).

levels for the lipogenic genes *scd1* and fatty acid synthase (*fas*) were increased significantly and non-significantly, respectively, in HFD mice, and E2 administration in HFD+E2 mice reduced expression levels of both genes (Figure 3A). Conversely, E2 treatment in the HFD+E2 group increased expression of the lipolytic gene adipose

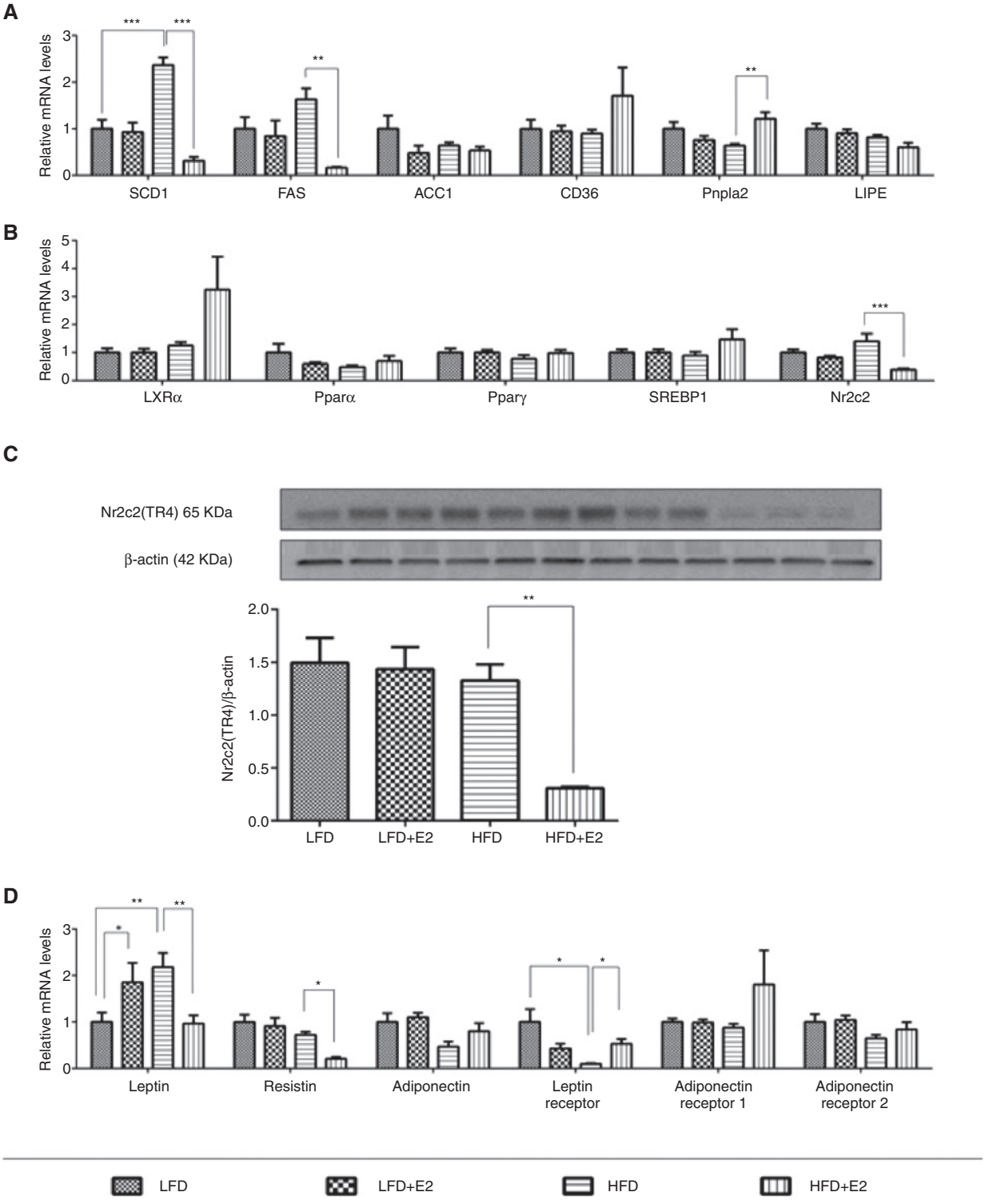

Figure 3: Expression of lipogenic genes, transcription factors, adipokines and adipokine receptors in visceral adipose from LFD and HFD mice treated with E2 or vehicle.

Total RNA was prepared from visceral adipose tissue dissected from vehicle- and E2-treated LFD and HFD mice and relative gene expression levels of lipogenic genes, transcription factors, and adipokines and adipokine receptors were assessed by real-time PCR (A, B and D, respectively). (C) Nr2c2/TR4 protein levels were assessed by Western blot. *, p-value < 0.05, **, p-value < 0.01 and ***, p-value < 0.001; n = 6 mice in (A), (B) and (D), and n = 3 mice in (C).

triglyceride lipase (*pnpla2*). Thus reduced visceral adipocyte hypertrophy in HFD+E2 mice was associated with reciprocal alterations in the expression of genes involved in fatty acid synthesis and triglyceride mobilization. In the LFD+E2 group, E2 treatment had no significant effect on any of these genes.

To understand how E2 altered lipogenic gene expression, the expression of transcription factors involved in its control was investigated. mRNA levels of neither *srebp1*, which regulates the expression of *scd1*, *fas* and acetyl-CoA carboxylase (*acc1*), nor of *lxrα*, which controls *srebp1* expression, were changed between the HFD and HFD+E2 groups (Figure 3B). Similarly, the expression levels of proliferator-activated receptor alpha (*pparα*), a regulator of fatty acid oxidation, and of *pparγ*, which activates genes involved in lipid uptake and adipogenesis, were unchanged in these groups. However, transcript levels of the nuclear receptor *nr2c2/tr4* were reduced in HFD+E2 mice (Figure 3B). Consistent with this, Nr2c2/TR4 protein levels were significantly reduced in the HFD+E2 group, compared with the HFD group, while there were no differences in Nr2c2/TR4 protein levels between the LFD and LFD+E2 groups (Figure 3C).

Studies of adipokine expression levels showed that leptin and adiponectin were significantly upregulated and non-significantly reduced, respectively, in HFD mice (Figure 3D). LFD+E2 mice exhibited increased leptin expression levels. Both leptin and resistin mRNAs were reduced in HFD+E2 mice, whilst adiponectin showed a tendency to increase (Figure 3D). Leptin receptor expression was reduced in HFD mice but increased in HFD+E2 mice.

Although the expression of *stat3*, which was identified previously as a direct target gene of E2, was unchanged in LFD+E2 mice, its expression was increased in HFD+E2 mice (Figure 4A). In addition to its role in adipokine signaling, Stat3 is also involved in regulation of the differentiation of brown adipose tissue [19], and so we examined the expression of the mitochondrial *ucp-1*. Expression of *ucp-1* was increased in HFD mice but was increased further in HFD+E2 mice (Figure 4A). Consistent with these observations, Western blotting showed that UCP-1 protein levels were significantly increased in HFD+E2 mice, compared with HFD mice (Figure 4B). Additionally, immunohistochemical staining for UCP-1 demonstrated an increased level of UCP-1 protein expression in adipose sections from HFD+E2 mice (Figure 4C). Furthermore, the expression of a second thermogenic gene, type II iodothyronine deiodinase (*dio-2*), was increased in HFD+E2 mice (Figure 4D). Despite this, the levels of mRNAs for peroxisome proliferator-activated receptor gamma coactivator 1-alpha (*pgc-1α*), a known driver of *ucp-1* expression, and of cell death-inducing DNA fragmentation factor (*cidea*) and cytochrome c oxidase subunit VIIIb (*cox-8b*), markers of brown adipocytes, were not altered. However, expression levels of *adrβ3*, which regulates *ucp-1* expression during the thermogenic response [24], were increased in HFD+E2 mice (Figure 4D). Expression levels of carnitine palmitoyltransferase 1b (*cpt-1b*), a brown adipose-specific gene involved in fatty acid utilization, were also increased in HFD+E2 mice.

Methylation status of SCD1, FAS, CPT-1b, DIO-2 and ADRβ3

To assess whether E2-induced expression changes were associated with epigenetic alterations in those genes, we assessed changes in methylation status at specific sites in several genes which were regulated by E2 in HFD mice, but not in LFD mice. There were no significant changes in the extent of methylation between the different groups with regard to the lipogenic genes *scd1* (Figure 5A) and *fas* (Figure 5B), nor for the brown adipose-specific gene *cpt-1b* (Figure 5C). However, HFD feeding resulted in increases in the extent of methylation of *adrβ3,* compared to LFD, whilst E2 decreased methylation levels significantly in HFD+E2 mice to levels comparable to those of the LFD and LFD+E2 groups (Figure 5D). Finally, E2 treatment in the HFD+E2 group significantly suppressed methylation levels in the *dio-2* gene, compared to HFD mice (Figure 5E).

Discussion

As a model of perimenopausal obesity and insulin resistance, HFD mice exhibited increased body weight, elevated plasma glucose values during an IPGTT, and raised fasting glucose levels [9]. This report demonstrated decreased plasma E2 levels in HFD mice, and treatment reconstituted E2 to levels comparable with 4 month-old animals [9]. The current study employed an identical E2 dosing regime, leading to reduced body weight and virtual normalization of insulin levels, fasting glucose and glucose tolerance. Indeed, E2 decreased body weight from 10 days of treatment, and this was preceded by reduced food intake from 4 days of treatment. Previous studies have shown that significant weight-reducing effects of E2 administration occur after only 1 week of E2 treatment [12, 25]. However, although the effects of E2 on body weight involve the regulation of food intake [11], ovariectomy has

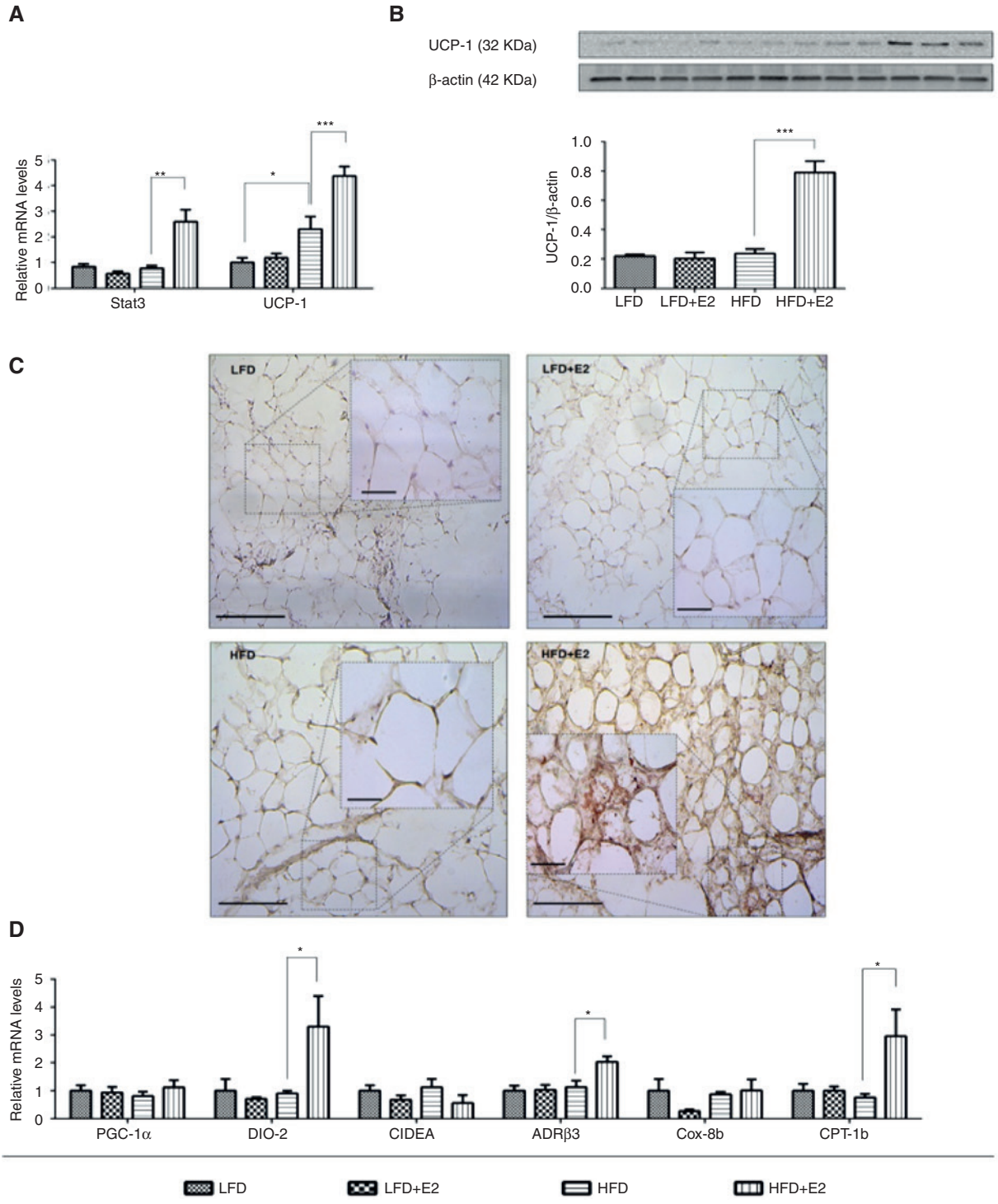

Figure 4: Expression of genes involved in the browning of visceral adipose in LFD and HFD mice treated with E2 or vehicle.
Total RNA was prepared from visceral adipose tissue dissected from vehicle- and E2-treated LFD and HFD mice, and real-time PCR was used to assess the relative expression levels of Stat 3 and UCP-1 (A) and brown adipose-specific genes (D). UCP-1 protein levels were assessed by Western blot (B) Immunohistochemical staining of visceral adipose sections for UCP-1 at 10× and 40× (C). *, p-value < 0.05, **, p-value < 0.01 and ***, p-value < 0.001; n = 6 mice in (A) and (D), and n = 3 mice in (B) and (C).

been shown to cause increased adiposity even after pair-feeding [12], suggesting that other mechanisms are also involved. As mentioned above, estrogen administration in ovariectomized mice leads to increases in energy expenditure [10], whilst ERKO and ARKO mice are obese in the absence of increased feeding [5, 6]. Although body weight

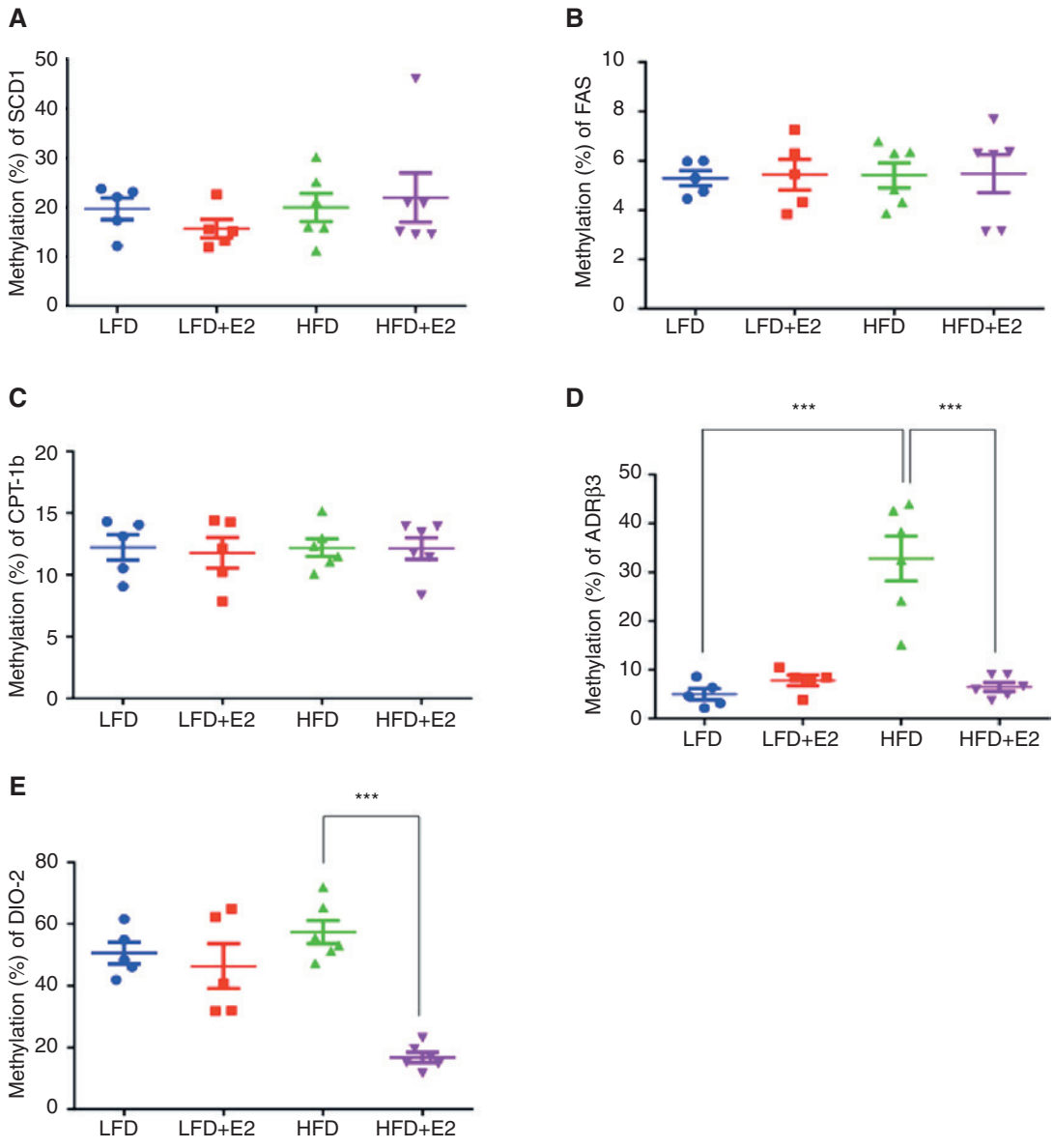

Figure 5: Methylation analyses of lipogenic and brown adipose-specific genes subject to differential regulation in visceral adipose tissue extracted from LFD and HFD mice treated with E2 or vehicle.
Analyses of methylation were carried out using an OneStep qMethyl Kit followed by real-time PCR, and the extent of methylation at each target sequence in the test reaction was expressed as a percentage of that target in the reference reaction; SCD1 (A), FAS (B), CPT-1b (C), ARβ3 (D) and DIO-2 (E), ***, p-value < 0.001; n = 5–6 mice.

in HFD+E2 mice continued to decrease throughout the course of E2 treatment, food consumption after 20 days of E2 treatment was not different from that in LFD animals, consistent with the proposal that the effects of E2 on body weight involve increased energy expenditure. As we did not employ pair-feeding in the current study, we cannot ascertain the extent to which reduced body weight in HFD+E2 mice was driven by decreased food intake.

We used MRI to quantify the proportions of total body volume occupied by the subcutaneous and visceral fat depots. Our MRI studies demonstrated an increase in the visceral adipose depot volume in HFD mice. Loss of visceral adipose volume in HFD+E2 mice paralleled body weight reduction in this group. There is a lack of studies of fat depot volume in aged mice which have been maintained on an HFD for extended time periods. However, MRI studies in 1-year-old female ARKO mice demonstrated an adipose tissue volume (predominantly the visceral and subcutaneous compartments) of 64.3% [6]. In the current study, the visceral and subcutaneous compartments

together account for 35% of body volume in HFD mice. Here, E2 reduced adiposity specifically in the abdominal compartment, in agreement with reports showing that E2 reduces abdominal adiposity in ovariectomized mice [26]. Similarly, ERT in postmenopausal women prevents the central distribution of body fat which occurs after menopause [27].

As E2 exerted its weight-reducing effects by regulating abdominal adiposity, we wished to assess whether adipocyte size was altered in this depot. Visceral adipocyte size was significantly increased in HFD mice, compared with adipocytes in LFD mice, whilst E2 treatment in HFD+E2 mice reduced adipocyte size and almost normalized this parameter to that seen in LFD mice. The reductions in visceral adipocyte size in HFD+E2 mice are comparable to those described previously in E2-treated ovariectomized mice [26]. As reduced adipocyte size correlates with increased insulin sensitivity [28, 29], E2-induced improvements in glucose tolerance are associated with the restoration of an insulin-sensitive phenotype in abdominal adipocytes. This is also consistent with our results showing glucose intolerance, whole-body insulin resistance and increased plasma levels of leptin and resistin in HFD mice, all of which were significantly improved by E2 treatment [9]. The mechanisms which underlie these anti-adipogenic effects of E2 are not clear. While both ERα and ERβ are expressed in adipose tissue [30], signaling through ERα is considered to dominate the effects of E2 in this tissue, which include the inhibition of fatty acid synthesis and the stimulation of lipolysis [31]. Meanwhile, studies in ovariectomized ERα-knockout mice demonstrate that signaling through ERβ is actually lipogenic [30] and may reduce insulin sensitivity via inhibition of PPARγ [17].

As adipocyte enlargement is associated with altered lipid metabolism [32], we assessed lipogenic and lipolytic gene expression in the same tissue samples that were employed for the morphological analyses. Increased adipocyte size in our model of perimenopausal obesity was associated with increased *scd1* expression, whilst E2-induced reductions in adipocyte size involved the reduced expression of *scd1* and *fas* and increased expression of adipose triglyceride lipase/*pnpla2*. These results suggest that reduced adipocyte size in HFD+E2 mice is associated with decreased adipogenesis, as seen previously [9]. The effects of E2 on lipogenic gene expression were not associated with alterations in the expression of *srebp1*, which we described previously in the adipose of E2-treated HFD mice [9]. However, this lack of concordance between the expression levels of *srebp1* and lipogenic genes has been reported before [33]. In addition, the expression of *lxrα*, which suppresses *srebp1* expression in adipose tissue [34], was also unchanged. Instead, the E2-induced suppression of lipogenic gene expression correlated with reductions in *nr2c2/tr4* expression at both mRNA and protein levels. This nuclear receptor *nr2c2/tr4* has recently been shown to be involved in the regulation of lipogenic gene expression which is inactivated by 5′-AMP-activated protein kinase (AMPK) [16], suggesting that it is a potentially important mediator of insulin sensitivity [35]. It was also notable that the effects of E2 on the expression of these lipogenic genes and transcription factors were specific to chronic HFD exposure, as E2 was without any effect on these genes in LFD+E2 mice.

The degree of adiposity correlates with leptin levels in both human subjects and rodent models [36, 37]. Here, leptin expression was increased in both LFD+E2 and HFD mice, whilst leptin receptor expression was reduced in the latter group. Plasma leptin levels are increased in HFD mice [9], and taken together, these features are reminiscent of leptin resistance in HFD mice [38]; indeed, reduced E2 levels have been associated with leptin insensitivity [39]. As we previously reported [9], improved glucose homeostasis in HFD+E2 mice was associated with reduced leptin expression and increased expression of the leptin receptor. In ovariectomized mice, E2 treatment has been shown to promote leptin sensitivity [40], and the possibility that leptin sensitivity is restored in HFD+E2 mice is consistent with the observed increases in *stat3* expression in HFD+E2 mice, as leptin is a known *stat3* activator, including in adipose tissue [41].

In addition, *stat3* is not only a target gene for E2 [18], but also its role in the regulation of brown adipocyte differentiation and function [19] suggested that elevated adipose *stat3* expression levels might be involved in the loss of adiposity in HFD+E2 mice via increased energy expenditure. Accordingly, we examined *ucp-1* expression in this tissue. Our observation of increased *ucp-1* expression in HFD+E2 mice was confirmed by the demonstration of both elevated UCP-1 protein levels and increased UCP-1 staining in the same tissue samples. The expression of UCP-1 contributes to the 'beiging' of white adipose depots which, although most frequently seen in the subcutaneous adipose depot, can also occur in the visceral adipose [42]. This process can be induced by stimuli such as cold exposure or exercise, and the ectopic induction of UCP-1 in response to hyperleptinemia has been described [43].

The increased levels of *ucp-1* expression in the visceral adipose of HFD+E2 mice led us to assess the expression of other brown adipocyte markers. Whilst the levels of mRNAs for *cidea*, *cox-8b* and of *pgc-1α*, a driver of *ucp-1* expression [44], were unchanged, the expression

of the thermogenic gene *dio-2* and that of *cpt-1b*, a brown adipose-specific gene involved in fatty acid utilization [45], were upregulated in HFD+E2 mice. Finally, our observation of increased *adrβ3* expression in HFD+E2 mice is consistent with the increased mRNA levels for *ucp-1* and *dio-2* described above. In white and brown adipocytes, ADRβ3 mediates the expenditure of energy and reductions in food intake which occur when mice are treated with a selective ADRβ3 agonist [46]. Also, the inhibition of ADRβ3 has been reported to impair the regulation of UCP-1, which in its turn leads to energy imbalance, obesity and insulin resistance [24]. Collectively, these results suggest the activation of genes in the visceral adipose tissue of HFD+E2 mice following 1 month of E2 treatment which are reminiscent of a brown adipocyte expression pattern. Although such 'beiging' of white adipose depots is most frequently seen in the subcutaneous depot, it has been observed in the visceral depot [42]. However, to our knowledge, this is the first time that E2 has been observed to increase the expression of brown adipose-specific markers in the visceral adipose depot and may provide an additional mechanism for E2-induced loss of adiposity.

Epigenetic events, via their regulation of chromatin structure and the transcriptional apparatus [47], may provide the link between environmental factors, such as diet, and the genetic alterations associated with obesity and insulin resistance, and HFD feeding has been associated with alterations in methylation at various locations within the genome [48]. In our study, E2 regulated the expression of a number of genes in the adipose of HFD mice, but not in LFD mice, raising the possibility that alterations in methylation status may affect the transcriptional activity of some genes targeted by E2. We did not observe alterations in the methylation status of *scd1*, *fas* and *cpt-1b*, although the expression of these genes was altered in HFD mice. This may be due to the fact that DNA methylation and gene expression do not correlate in all circumstances [49]. However, the upregulation of expression levels of *adrβ3* and *dio-2* by E2 treatment in HFD+E2 mice was correlated with the suppression of methylation levels in these genes. As the methylation at specific promoter and/or enhancer sites within genes is associated with decreased transcriptional activity of those genes due to decreased transcription factor binding [50], our results support the possibility that the effects of E2 on *adrβ3* and *dio-2* expression levels in adipose tissue may involve the regulation by E2 of epigenetic modifications within these genes.

In conclusion, improvements in glucose homeostasis and weight loss due to E2 treatment in this mouse model of perimenopausal obesity and insulin resistance are associated with the suppression of visceral adiposity and reductions in visceral adipocyte size. These events in visceral adipocytes involve reduced lipogenesis, augmented fatty acid utilization and the activation of brown adipose tissue-specific gene expression. This latter process may involve E2-dependent alterations in epigenetic modifications which confer transcriptional accessibility to these genes.

Acknowledgments: This study was supported by grants from Department of Pathology, College of Medicine, Najran University Hospital and Najran University, Saudi Arabia. The invaluable technical expertise of Yvonne Strömberg and Katalin Benedek is gratefully acknowledged. The authors would also like to thank Florian Salomons for his help during the MRI image analyses. We are also grateful for the financial support from the Konung Gustaf V's och Drottning Victorias Frimurarestiftelse, the Swedish Research Council, the Family Erling-Persson Foundation, the Novo Nordisk Foundation, the Stichting af Jochnick Foundation, the Swedish Diabetes Association, the Scandia Insurance Company Ltd., the Diabetes Research and Wellness Foundation, Berth von Kantzow's Foundation, the Strategic Research Program in Diabetes at Karolinska Institutet, the ERC-2013-AdG 338936-Betalmage, the Swedish Foundation for Strategic Research, and the Knut and Alice Wallenberg Foundation.

Author Statement

Funding: This study was supported by grants from Department of Pathology, College of Medicine, Najran University Hospital and Najran University, Saudi Arabia. We are also grateful for the financial support from the Konung Gustaf V's och Drottning Victorias Frimurarestiftelse, the Swedish Research Council, the Family Erling-Persson Foundation, the Novo Nordisk Foundation, the Stichting af Jochnick Foundation, the Swedish Diabetes Association, the Scandia Insurance Company Ltd., the Diabetes Research and Wellness Foundation, Berth von Kantzow's Foundation, the Strategic Research Program in Diabetes at Karolinska Institutet, the ERC-2013-AdG 338936-Betalmage, the Swedish Foundation for Strategic Research, and the Knut and Alice Wallenberg Foundation.

Conflict of interest: Authors state no conflict of interest.

Informed consent: Informed consent is not applicable.

Ethical approval: The research related to use of animals has been in compliance with all the relevant national regulations and institutional policies for the care and use of animals.

References

1. Lovejoy JC, Champagne CM, de Jonge L, Xie H, Smith SR. Increased visceral fat and decreased energy expenditure during the menopausal transition. Int J Obesity 2008;32:949–58.
2. Carey DG, Jenkins AB, Campbell LV, Freund J, Chisholm DJ. Abdominal fat and insulin resistance in normal and overweight women: direct measurements reveal a strong relationship in subjects at both low and high risk of NIDDM. Diabetes 1996;45:633–8.
3. Decode Study Group. Age- and sex-specific prevalences of diabetes and impaired glucose regulation in 13 European cohorts. Diabetes Care 2003;26:61–9.
4. Kanaya AM, Herrington D, Vittinghoff E, Lin F, Grady D, Bittner V, Cauley JA, Barrett-Connor E, Heart, Estrogen/progestin Replacement S. Glycemic effects of postmenopausal hormone therapy: the Heart and Estrogen/progestin Replacement Study. A randomized, double-blind, placebo-controlled trial. Ann Intern Med 2003;138:1–9.
5. Heine PA, Taylor JA, Iwamoto GA, Lubahn DB, Cooke PS. Increased adipose tissue in male and female estrogen receptor-alpha knockout mice. Proc Natl Acad Sci USA 2000;97:12729–34.
6. Jones ME, Thorburn AW, Britt KL, Hewitt KN, Wreford NG, Proietto J, Oz OK, Leury BJ, Robertson KM, Yao S, Simpson ER. Aromatase-deficient (ArKO) mice have a phenotype of increased adiposity. Proc Natl Acad Sci USA 2000;97:12735–40.
7. Ribas V, Nguyen MT, Henstridge DC, Nguyen AK, Beaven SW, Watt MJ, Hevener AL. Impaired oxidative metabolism and inflammation are associated with insulin resistance in ERalpha-deficient mice. Am J Physiol Endoc Metab 2010;298:E304–19.
8. Clegg DJ, Brown LM, Woods SC, Benoit SC. Gonadal hormones determine sensitivity to central leptin and insulin. Diabetes 2006;55:978–87.
9. Bryzgalova G, Lundholm L, Portwood N, Gustafsson JA, Khan A, Efendic S, Dahlman-Wright K. Mechanisms of antidiabetogenic and body weight-lowering effects of estrogen in high-fat diet-fed mice. Am J Physiol Endoc Metab 2008;295:E904–12.
10. Musatov S, Chen W, Pfaff DW, Mobbs CV, Yang XJ, Clegg DJ, Kaplitt MG, Ogawa S. Silencing of estrogen receptor alpha in the ventromedial nucleus of hypothalamus leads to metabolic syndrome. Proc Natl Acad Sci USA 2007;104:2501–6.
11. Liang YQ, Akishita M, Kim S, Ako J, Hashimoto M, Iijima K, Ohike Y, Watanabe T, Sudoh N, Toba K, Yoshizumi M, Ouchi Y. Estrogen receptor beta is involved in the anorectic action of estrogen. Int J Obes Relat Metab Disord 2002;26:1103–9.
12. Roy EJ, Wade GN. Role of food intake in estradiol-induced body weight changes in female rats. Horm Behav 1977;8:265–74.
13. Stubbins RE, Holcomb VB, Hong J, Nunez NP. Estrogen modulates abdominal adiposity and protects female mice from obesity and impaired glucose tolerance. Eur J Nutr 2012;51:861–70.
14. Horton JD, Goldstein JL, Brown MS. SREBPs: activators of the complete program of cholesterol and fatty acid synthesis in the liver. J Clin Invest 2002;109:1125–31.
15. Korach-Andre M, Archer A, Gabbi C, Barros RP, Pedrelli M, Steffensen KR, Pettersson AT, Laurencikiene J, Parini P, Gustafsson JA. Liver X receptors regulate de novo lipogenesis in a tissue-specific manner in C57BL/6 female mice. Am J Physiol Endoc Metab 2011;301:E210–22.
16. Kim E, Liu NC, Yu IC, Lin HY, Lee YF, Sparks JD, Chen LM, Chang C. Metformin inhibits nuclear receptor TR4-mediated hepatic stearoyl-CoA desaturase 1 gene expression with altered insulin sensitivity. Diabetes 2011;60:1493–503.
17. Foryst-Ludwig A, Clemenz M, Hohmann S, Hartge M, Sprang C, Frost N, Krikov M, Bhanot S, Barros R, Morani A, Gustafsson JA, Unger T, Kintscher U. Metabolic actions of estrogen receptor beta (ERbeta) are mediated by a negative cross-talk with PPAR-gamma. PLoS Genet 2008;4:e1000108.
18. Gao H, Bryzgalova G, Hedman E, Khan A, Efendic S, Gustafsson JA, Dahlman-Wright K. Long-term administration of estradiol decreases expression of hepatic lipogenic genes and improves insulin sensitivity in ob/ob mice: a possible mechanism is through direct regulation of signal transducer and activator of transcription 3. Mol Endocrinol 2006;20:1287–99.
19. Derecka M, Gornicka A, Koralov SB, Szczepanek K, Morgan M, Raje V, Sisler J, Zhang Q, Otero D, Cichy J, Rajewsky K, Shimoda K, Poli V, Strobl B, Pellegrini S, Harris TE, Seale P, Russell AP, McAinch AJ, O'Brien PE, Keller SR, Croniger CM, Kordula T, Larner AC. Tyk2 and Stat3 regulate brown adipose tissue differentiation and obesity. Cell Metab 2012;16:814–24.
20. Monjo M, Rodriguez AM, Palou A, Roca P. Direct effects of testosterone, 17 beta-estradiol, and progesterone on adrenergic regulation in cultured brown adipocytes: potential mechanism for gender-dependent thermogenesis. Endocrinology 2003;144:4923–30.
21. Chaplin A, Palou A, Serra F. Methylation analysis in fatty-acid-related genes reveals their plasticity associated with conjugated linoleic acid and calcium supplementation in adult mice. Eur J Nutr 2015;1–13.
22. Maples JM, Brault JJ, Witczak CA, Park S, Hubal MJ, Weber TM, Houmard JA, Shewchuk BM. Differential epigenetic and transcriptional response of the skeletal muscle carnitine palmitoyltransferase 1B (CPT1B) gene to lipid exposure with obesity. Am J Physiol Endoc Metab 2015;309:E345–56.
23. Kurylowicz A, Jonas M, Lisik W, Jonas M, Wicik ZA, Wierzbicki Z, Chmura A, Puzianowska-Kuznicka M. Obesity is associated with a decrease in expression but not with the hypermethylation of thermogenesis-related genes in adipose tissues. J Transl Med 2015;13:31.
24. Klein J, Fasshauer M, Benito M, Kahn CR. Insulin and the beta3-adrenoceptor differentially regulate uncoupling protein-1 expression. Mol Endocrinol 2000;14:764–73.
25. Mohamed MK, Abdel-Rahman AA. Effect of long-term ovariectomy and estrogen replacement on the expression of estrogen receptor gene in female rats. Eur J Endocrinol 2000;142:307–14.
26. Yonezawa R, Wada T, Matsumoto N, Morita M, Sawakawa K, Ishii Y, Sasahara M, Tsuneki H, Saito S, Sasaoka T. Central versus peripheral impact of estradiol on the impaired glucose metabolism in ovariectomized mice on a high-fat diet. Am J Physiol Endoc Metab 2012;303:E445–56.
27. Gambacciani M, Ciaponi M, Cappagli B, Piaggesi L, De Simone L, Orlandi R, Genazzani AR. Body weight, body fat distribution, and hormonal replacement therapy in early postmenopausal women. J Clin Endocrinol Metab 1997;82:414–7.
28. Bauche IB, El Mkadem SA, Pottier AM, Senou M, Many MC, Rezsohazy R, Penicaud L, Maeda N, Funahashi T, Brichard SM. Overexpression of adiponectin targeted to adipose tissue in transgenic mice: impaired adipocyte differentiation. Endocrinology 2007;148:1539–49.

29. Roberts R, Hodson L, Dennis AL, Neville MJ, Humphreys SM, Harnden KE, Micklem KJ, Frayn KN. Markers of de novo lipogenesis in adipose tissue: associations with small adipocytes and insulin sensitivity in humans. Diabetologia 2009;52:882–90.
30. Naaz A, Zakroczymski M, Heine P, Taylor J, Saunders P, Lubahn D, Cooke PS. Effect of ovariectomy on adipose tissue of mice in the absence of estrogen receptor alpha (ERalpha): a potential role for estrogen receptor beta (ERbeta). Horm Metab Res 2002;34:758–63.
31. Hansen FM, Fahmy N, Nielsen JH. The influence of sexual hormones on lipogenesis and lipolysis in rat fat cells. Acta Endocrinol 1980;95:566–70.
32. Bluher M, Wilson-Fritch L, Leszyk J, Laustsen PG, Corvera S, Kahn CR. Role of insulin action and cell size on protein expression patterns in adipocytes. J Biol Chem 2004;279:31902–9.
33. Kang EJ, Lee JE, An SM, Lee JH, Kwon HS, Kim BC, Kim SJ, Kim JM, Hwang DY, Jung YJ, Yang SY, Kim SC, An BS. The effects of vitamin D3 on lipogenesis in the liver and adipose tissue of pregnant rats. Int J Mol Med 2015;36:1151–8.
34. Yoshikawa T, Shimano H, Amemiya-Kudo M, Yahagi N, Hasty AH, Matsuzaka T, Okazaki H, Tamura Y, Iizuka Y, Ohashi K, Osuga J, Harada K, Gotoda T, Kimura S, Ishibashi S, Yamada N. Identification of liver X receptor-retinoid X receptor as an activator of the sterol regulatory element-binding protein 1c gene promoter. Mol Cell Biol 2001;21:2991–3000.
35. Lin SJ, Zhang Y, Liu NC, Yang DR, Li G, Chang C. Minireview: pathophysiological roles of the TR4 nuclear receptor: lessons learned from mice lacking TR4. Mol Endocrinol 2014;28:805–21.
36. Frederich RC, Hamann A, Anderson S, Lollmann B, Lowell BB, Flier JS. Leptin levels reflect body lipid content in mice: evidence for diet-induced resistance to leptin action. Nat Med 1995;1:1311–4.
37. Maffei M, Halaas J, Ravussin E, Pratley RE, Lee GH, Zhang Y, Fei H, Kim S, Lallone R, Ranganathan S, Kern PA, Friedman JM. Leptin levels in human and rodent: measurement of plasma leptin and ob RNA in obese and weight-reduced subjects. Nat Med 1995;1:1155–61.
38. Sainz N, Barrenetxe J, Moreno-Aliaga MJ, Martinez JA. Leptin resistance and diet-induced obesity: central and peripheral actions of leptin. Metab Clin Exp 2015;64:35–46.
39. Ainslie DA, Morris MJ, Wittert G, Turnbull H, Proietto J, Thorburn AW. Estrogen deficiency causes central leptin insensitivity and increased hypothalamic neuropeptide Y. Int J Obes Relat Metab Disord 2001;25:1680–8.
40. Brown LM, Clegg DJ. Central effects of estradiol in the regulation of food intake, body weight, and adiposity. J Steroid Biochem Mol Biol 2010;122:65–73.
41. Kim YB, Uotani S, Pierroz DD, Flier JS, Kahn BB. In vivo administration of leptin activates signal transduction directly in insulin-sensitive tissues: overlapping but distinct pathways from insulin. Endocrinology 2000;141:2328–39.
42. Barbatelli G, Murano I, Madsen L, Hao Q, Jimenez M, Kristiansen K, Giacobino JP, De Matteis R, Cinti S. The emergence of cold-induced brown adipocytes in mouse white fat depots is determined predominantly by white to brown adipocyte transdifferentiation. Am J Physiol Endoc Metab 2010;298:E1244–53.
43. Okamatsu-Ogura Y, Uozumi A, Toda C, Kimura K, Yamashita H, Saito M. Uncoupling protein 1 contributes to fat-reducing effect of leptin. Obes Res Clin Pract 2007;1:223–90.
44. Barbera MJ, Schluter A, Pedraza N, Iglesias R, Villarroya F, Giralt M. Peroxisome proliferator-activated receptor alpha activates transcription of the brown fat uncoupling protein-1 gene. A link between regulation of the thermogenic and lipid oxidation pathways in the brown fat cell. J Biol Chem 2001;276:1486–93.
45. Brown NF, Hill JK, Esser V, Kirkland JL, Corkey BE, Foster DW, McGarry JD. Mouse white adipocytes and 3T3-L1 cells display an anomalous pattern of carnitine palmitoyltransferase (CPT) I isoform expression during differentiation. Inter-tissue and inter-species expression of CPT I and CPT II enzymes. Biochem J 1997;327(Pt 1):225–31.
46. Grujic D, Susulic VS, Harper ME, Himms-Hagen J, Cunningham BA, Corkey BE, Lowell BB. Beta3-adrenergic receptors on white and brown adipocytes mediate beta3-selective agonist-induced effects on energy expenditure, insulin secretion, and food intake. A study using transgenic and gene knockout mice. J Biol Chem 1997;272:17686–93.
47. Jones PA, Takai D. The role of DNA methylation in mammalian epigenetics. Science 2001;293:1068–70.
48. Milagro FI, Campión J, García-Díaz DF, Goyenechea E, Paternain L, Martínez JA. High fat diet-induced obesity modifies the methylation pattern of leptin promoter in rats. J Physiol Biochem 2009;65:1–9.
49. Eckhardt F, Lewin J, Cortese R, Rakyan VK, Attwood J, Burger M, Burton J, Cox TV, Davies R, Down TA, Haefliger C, Horton R, Howe K, Jackson DK, Kunde J, Koenig C, Liddle J, Niblett D, Otto T, Pettett R, Seemann S, Thompson C, West T, Rogers J, Olek A, Berlin K, Beck S. DNA methylation profiling of human chromosomes 6, 20 and 22. Nat Genet 2006;38:1378–85.
50. Medvedeva YA, Khamis AM, Kulakovskiy IV, Ba-Alawi W, Bhuyan MS, Kawaji H, Lassmann T, Harbers M, Forrest AR, Bajic VB. Effects of cytosine methylation on transcription factor binding sites. BMC Genomics 2014;15:119.